Field Emission Investigation in a 3.6 GHz SRF Cavity using X-Ray Measuring Systems

M. Fouaidy, T. Junquera, S. Bousson

Institut de Physique Nucléaire (CNRS-IN2P3 - Univ. Paris XI). 91406 ORSAY France

Abstract

A special SRF Niobium cavity operating at 3.6 GHz in the TM020 mode has been designed for Field Emission studies and successfully tested. A maximum peak surface electric field E_{pk} = 95 MV/m limited by the total available RF power of 20 W with a low field unloaded quality factor $Q0 \cong 5.10^9$ was reproducibly reached. Heavy FE was observed for a peak surface electric field $E_{pk} \geq 40$ MV/m.

This FE electron loading was investigated using different diagnostic systems : electron current probe, FE induced X-rays intensity mapping system (Scanning Photodiodes) and a NaI detector for X-rays spectrum analysis purpose. Primary FE electron trajectories are calculated and stable emission sites leading to the observed X-rays maps hot spots (i.e. Bremsstrahlung X-radiation induced by FE electrons impact on the Nb RF surface) are successfully located for different experimental run conditions. The measured X-rays spectra are in good agreement with the numerical simulation results hence allowing a good calibration of the peak surface electric field by comparison to the electromagnetic fields distribution computed with the URMEL code .

I. INTRODUCTION

SRF cavities are a very promising technology for the future electon-positron colliders [1, 2]. However the TESLA design goals (Accelerating electric field E_{acc} = 25 MV/m, unloaded quality factor Q_0 = 5.10^9 at 1.8 K) are mainly limited by two anomalous RF losses of the accelerating cavities (9 cells, f = 1.3 GHz) : dielectric / magnetic losses at the RF surface defects or contaminants which could induce the cavity Thermal Breakdown, and Field Emission (FE) or electron loading which consume extra RF power, degradates drastically the cavity Q_0 and could also cause Thermal Breakdown. In order to investigate FE physical origin and to progress in the basic understanding of this phenomena, we developed a special apparatus dedicated to this purpose. We present in this paper the first results obtained with our experimental setup. These experimental data are analysed and successfully compared to the numerical simulation results. The method used allows us to perform a precise calibration of the surface electric field by comparison to the results computed by the URMEL code .

II. EXPERIMENTAL SETUP

The bulk niobium SRF cavity used (Fig. 1) was specially designed for FE studies. It is mainly based on an accelerating 1.5 GHz half-cell high purity (RRR ≥ 130) Nb cavity closed at the equator with a Nb plate EB welded to the cavity body. This cavity shape and the use of the TM 020 operating mode (see below) is interesting in two respects : a) the high peak surface electric field region (i.e $E_{pk} \geq 0.80 E_{pk}^{max}$) is limited to a small disk (Ø 30mm) of the cavity bottom central region, b) it offers the possibility of in-situ vizualisation (i.e optical measurements) of this potentialy electron field emitting area. Moreover, in order to enhance the surface electric field in the area to be investigated (cavity bottom central region), a dimple (radius : 13 mm, height : 6 mm) was put at this location : an enhancement factor of 2.5, with respect to the flat bottom cavity, is expected from the URMEL code calculations.

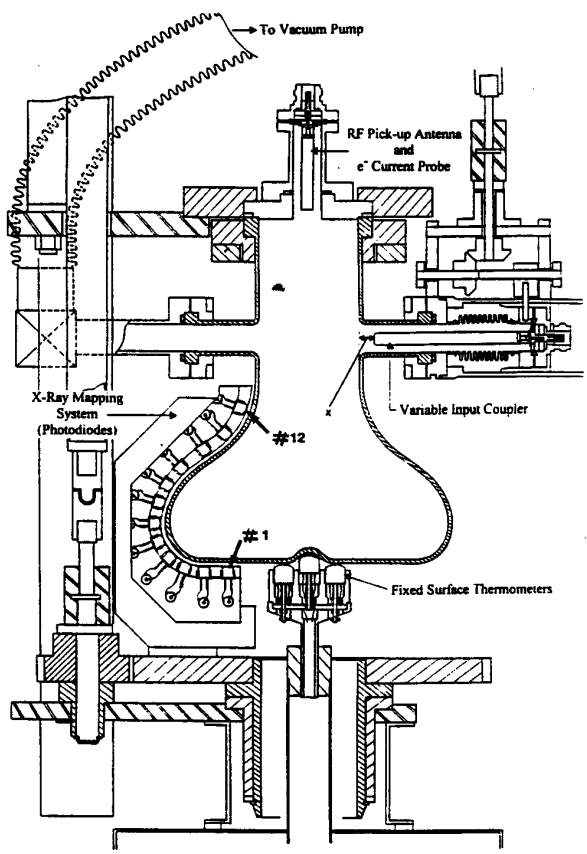

Fig. 1 : Cross-section of the "bottle"-like SRF cavity with the scanning photodiodes arm (x-rays mapping system) and the fixed thermometric array

More precisely the cavity bottom was embossed by cold plastic deformation. Then the cavity was heat treated in a

vacuum furnace in 3 stages to restore the RRR : fast temperature increase from T_i = 300 K to T_f = 670 K then hold at T_f during 1 hour, this process was repeated twice from T_i = 670K to T_f = 920K then from T_i = 920K to T_f = 1020K. Finally the cavity was chemically etched (4µm) using the standard acid mixture (HF:HNO3:H_3PO_4, 1:1:1), rinsed with demineralized pure water and dried under dust free laminar flux then keeped under pure nitrogen gas atmosphere for the transport to the test stand. Notice that the cavity was chemically etched (30µm) pure water rinsed and cold RF tested before being embossed.

A variable main RF coupler, a mechanical device attached to it, a stepping motor and an electronic system has been used so as to enable optimum RF coupling of the TWT to the cavity. This system allows us to have a good external coupling Q_{ext} in the range $9.4.10^7 \leq Q_{ext} \leq 1.6.10^{10}$ when x is varied from 3 mm to 13 mm).

A titanium RF probe is used to monitor the RF power transmitted into the cavity and alternately to collect FE electrons current (primary and secondary electrons) by the use of RF/DC diplexers : in the later case (i.e electron current monitoring), a DC bias voltage (10 V) could be applied to this probe. Different devices are used as FE and anomalous RF losses diagnostic probes : an array of 7 fixed HeII-cooled surface thermometers [3], a rotating arm of 12 BPX66 photodiodes (Scanning Photodiodes Arm : S.Ph.A) with amplifiers developed in the Lab. for measuring X radiations intensity (X-rays maps) induced by FE electrons impacting on the cavity RF surface and a X-rays spectrometer (NaI crystal detector).

The photodiodes were carefully calibrated [4] prior to the RF tests using a Van de Graaf Accelerator : they were placed in front of a 2 mm thick Niobium sheet target bombarded by an electron beam with an intensity I_{e^-} and an energy E_{e^-} in the usefull range (i.e 300 nA $\leq I_{e^-} \leq$ 2µA and 0.75 MeV $\leq E_{e^-} \leq$ 2.5 MeV).

Mode	Freq. (MHz)	E_{pk} / √U MV/m/√ J	H_{pk} / E_{pk} A/MV
TM 010	1661	665.6	7.2 10^{-4}
TM 020	3554	1278.3	8.1 10^{-4}

Table 1 : Comparison of the RF characteristics of the TM010 and TM020 modes as computed with the URMEL code.

The Table 1 resulting from URMEL [5] code calculations shows clearly that the TM020 mode is the best one according to the following criteria : high E_{pk} at the central region of the cavity bottom for a given RF power into the cavity (P_{cav}) low value of the ratio H_{pk}/E_{pk} of the peak surface magnetic field H_{pk} to E_{pk} so as to reduce the Joule heating.

III. EXPERIMENTAL RESULTS AND DISCUSSION

A. Unloaded quality factor and surface resistance

On Figure 2, we show the unloaded quality factor Q_0 versus the maximum peak surface electric field E_Z (i.e at the cavity dimple top location) at a bath temperature T_{bath} = 1.8K in the TM 020 mode (f = 3.55 GHz).

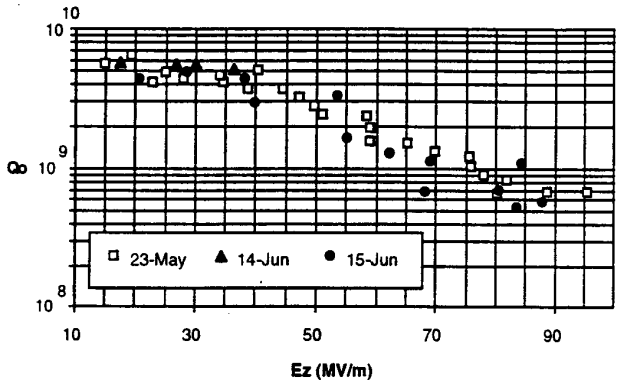

Fig. 2 : Unloaded quality factor Q0 vs the maximum peak surface electric field Ez at the dimple top for 3 different runs (TM 020 mode, f ≅ 3.6 Ghz) (T_{bath} ≅ 1.8 K)

The highest achieved surface electric field $E_Z \cong$ 95 MV/m was limited by the maximum available RF power (≅ 20 W). The low field Q_0 value at $T_{bath} \cong$ 1.8 K in the TM 020 mode was around 5.10^9, leading to a total surface resistance R_S = 84 nΩ : the corresponding geometric factor as calculated from the URMEL results is G = 427 Ω. The observed strong Q_0 decrease for $E_Z \geq$ 40 MV/m is due to FE electron loading. Notice that several RF tests were performed in the course of the experiments and the recorded Q_0 vs E_Z results show a good reproducibility : the difference between two experimental data sets did not exceed 30%, while the cavity was warmed up from 1.8 K to 300 K and cooled down again between two succesive runs but without breaking the vacuum. Finally, the low field Q_0 values were recorded versus T_{bath} from 4.2 K down to 1.8 K. The resulting total surface resistance R_S vs T_{bath} data was fitted according to the well known relation :

$$R[n\Omega] = \frac{A.f[GHz]^2}{T_{bath}[K]}.\exp\left(\frac{-B}{T_{bath}[K]}\right) + R_{res}$$

These experimental data are displayed in Figure 3 in terms of $y = \ln[(G/Q_0)-R_{res}).T_{bath} / f^2]$ vs $1/T_{bath}$ along with the fit curve which was optimum for R_{res} = 52 nΩ : as expected the resulting fit curve is a straight line with a slope B = -17.98 K and an intercept ln (A) = 11.51 on the y-axis at x = 0. These fitted values of A and B are in agreement with those previousely reported (i.e B =-18K , ln (A) = 11.71 = ln(10^5)) by other authors [6] for the commercialy available Niobium.

The actually measured residual surface resistance of 52 nΩ seems to be a good RF performance if one considers the special cavity geometry : obviously, this shape (i.e 'bottle' like) is not well suited for SRF surface preparation (i.e chemical etching, pure water rinsing, drying...etc).

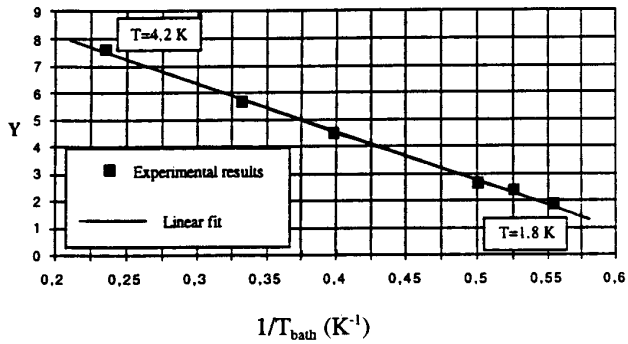

Fig. 3 : Bath temperature dependence of the surface resistance in the TM020 mode. A good fit is obtained for R_{res} = 52 nΩ

Moreover, our residual surface resistance value of 52 nΩ is about a factor 2 lower than that obtained by the Cornell SRF group [7] with the same shape but smaller cavity operated also in the TM020 mode at a higher frequency (f = 5.8 GHz) than our cavity.

B. X-rays data analysis

Interesting informations can be drawn from the X-rays data analysis. The main objective is to determine the location of electrons emitting sites and also to verify the consistency between experimental data and simulated results for the electromagnetic fields calibration factor K_E in the relation $E_Z = K_E (P_{cav}.Q_0)^{1/2}$. Data that are needed to achieve these goals are FE electrons impact locations and also landing electrons kinetic energy at the corresponding hot spots (i.e intense X-rays emission). The Scanning Photodiodes Arm provides us with X-rays emitter sites location (i.e. electrons impact locations) in terms of the cylindrical coordinates φ, r and z : φ the meridian position of the S.Ph.A in the radial (r) and the axial (z) directions by the X-rays sensor geographic location on the S.Ph.A (i.e photodiode number).

The NaI detector allows us to determine electrons energy : X-rays are emitted by Bremsstrahlung when the FE electrons hit and penetrate into the cavity wall. The result is a X-rays spectrum which wavelengh depends on how much the impacting electrons was slowed-down into the Nb sheet before emitting the X-rays.

This NaI detector calibration (Co and Cs radioactive sources [8]) prior to the RF tests, allows us to measure X-rays energy to within 20 keV.

A typical X-rays intensity map recorded by the photodiodes is given in Figure 4.

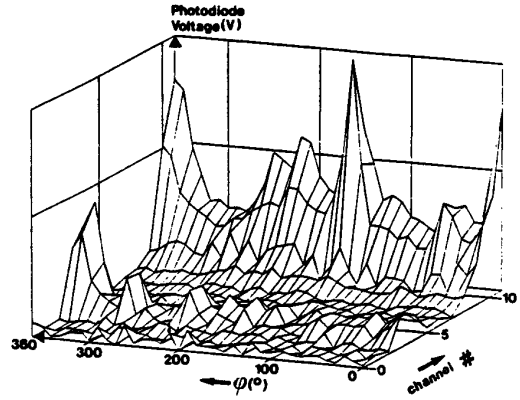

Fig. 4 : X-Rays intensity map recorded by the S.Ph.A for $E_z \approx 90 \pm 10$MV/m (run of 15.06.95)

This map was taken at an electric field $E_z \approx 90$ MV/m. Notice that an another X-rays map was recorded at E_z = 83 MV/m (run of May 23, 1995) the cavity being warmed up from 1.8 K to 300 K without breaking the vacuum between the two tests. These maps clearly show the stability of the strongest observed electron emitter over a period of 3 weeks. The two major hot spots are located at the meridians φ = 210° and φ = 150°, at the photodiodes #12 and #11 locations (channel #11 and #10). According to these results, we placed our NaI detector in front of the photodiode #12, just outside the cryostat, to face the hot spot.

An example of a X-rays spectrum for an other run (E_Z = 72 MV/m) is shown in Figure 5.

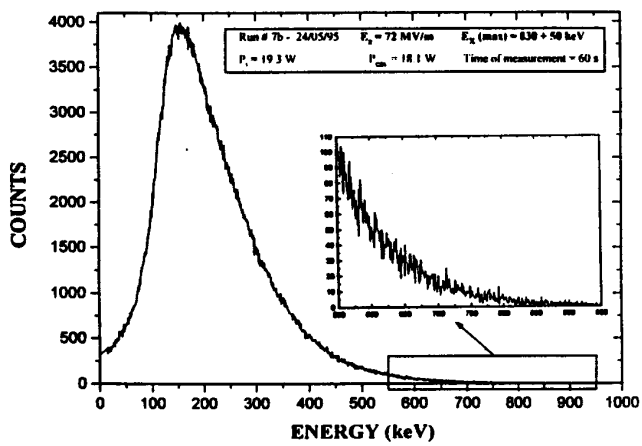

Fig. 5 : X-Rays spectra induced by FE impacting electrons on the cavity RF surface for two runs at different E_z

Since the X-rays emission intensity was high, 60 s was sufficient to perform precise measurements : the background intensity was very low (10 counts maximum) as compared to the 4000 counts recorded at the peak center hence allowing us to obtain nearly 50 keV precision for the maximum X-rays energy measurement. At E_z = 57 MV/m the maximum X-rays energy (spectrum tail) was 580 ± 40 keV, and at

E_Z = 72 MV/m, we measured 830 ± 50 keV. Finally we measured with a ionization chamber positionned near the NaI crystal an activity of 400 mrad/h at E_z = 72 MV/m.

Both informations (hot spot location and impacting electrons energy) were necessary for locating the emitter source via electrons trajectories calculations.

C. Field Emitted electrons trajectories calculations

Field Emitted electron trajectories were calculated using the electromagnetic fields distribution (TM020 mode) computed with the URMEL code as input file. Notice that only primary electron are taken into account in the numerical simulation results here presented : neither back-scattered electrons nor secondary emitted electrons are concerned. In all the following, the electron trajectories calculation are performed assuming a negligible electron energy at their emission which is a good approximation. A trajectory family is calculated for different emission phases (ϕ) with respect to the electric RF field : $E = E_{pk} \sin(\omega t+\phi)$. Each trajectory family is characterized by four parameters : the emitter source location (S_0), the peak surface electric field at the dimple top E_Z, the field enhancement factor β (beta) and the emitting area (SURF). Obviously, the last two parameters have no influence on electron trajectories, neither on impacting electron kinetic energy nor on the resulting shape of the impacting power distribution (dP/dS) vs S. Howewer, the emitted electron current and the magnitude of dP/dS depend exponentially on β (Fowler-Nordeim relation).

We performed these trajectories calculations with the same conditions as in our experiments. We made systematic numerical runs, changing the emitter location until we found results on X-rays emission sites and on impacting electrons energy that are consistent with the experimental data.

For an emitter located at the curvilinear coordinate S_0 = 0.42 cm (about the dimple half height), a good agreement between experiments and simulations was found.

The computed results with E_Z = 72 MV/m are plotted in Figures 6a, 6b and 6c. For this numerical run, we present : the primary FE electrons trajectories (Fig. 6a), the simulated X-rays emission intensity (Fig. 6b) and the simulated distribution of the power deposited by the impacting electrons (Fig. 6c). The electron trajectrories, which depend on ϕ are computed with a step of 1 degree from 190 to 350 degree (but displayed each 10 degrees). The run conditions are : SURF = 10^{-9} cm^2, β = 140, ESURF = E_z (peak surface field at the dimple top), EPK (peak surface field at the emitter location S_0). The result PUISS.MOY (in Watt) is the total mean dissipated power by impacting electrons, averaged over an RF period in the range of the considered phase interval.

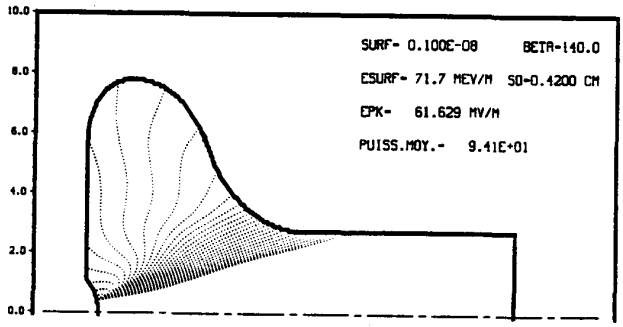

Fig. 6a

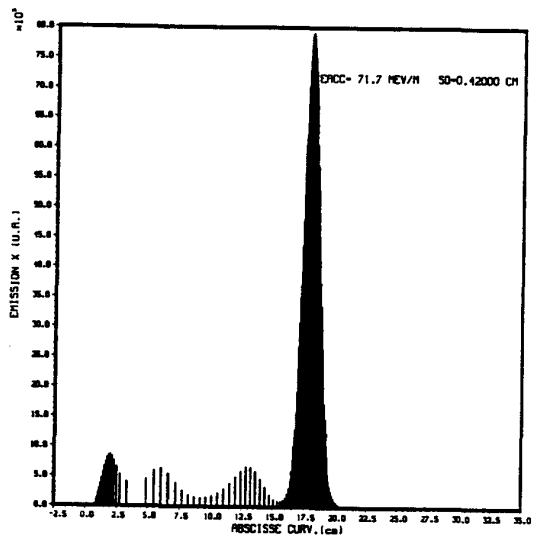

Fig. 6b

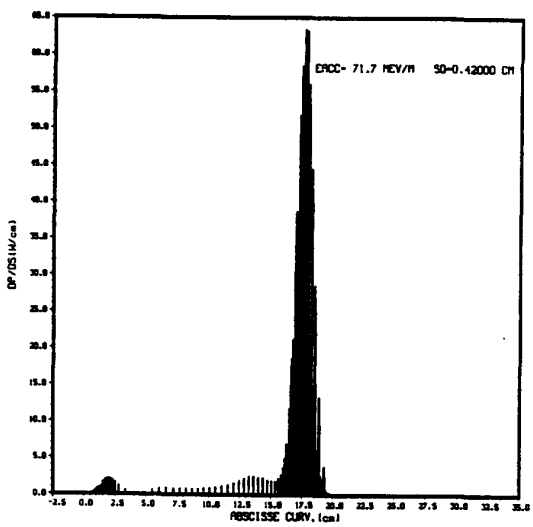

Fig 6c

Simulations results on primary impacting electrons energy are also in agreement with experimental results on the maximum X-rays energy (Table 2) for the two runs (E_z = 57MV/m and E_z = 72MV/m. Notice that the whole results with E_z = 57MV/m (i.e. trajectories, dp/ds,..) are not displayed.

E_z (MV/m)	E_{RX} (keV)	E_{e^-} (keV)
57	580 ± 40	620
72	830 ± 50	842

Table 2 : Comparison between experimental E_{RX} and simulated E_{e^-} impacting electrons energy.

IV. CONCLUSION AND FUTURE ISSUES

The TM 020 3.6 GHz "bottle" like SRF Nb cavity specially designed for FE studies was successfully tested with all its X-rays diagnostic systems (scanning photo diodes and NaI spectrometer). We achieved reproducibly a maximum peak surface electric field at the dimple top E_{pk} = 95 MV/m, limited only by the available RF power (20 W). The measured residual surface resistance was sufficiently low (52 nΩ) if one considers the special cavity shape. The X-rays diagnostic system together with FE electrons trajectories calculations allow us to locate precisely FE sites and hence to carefully calibrate E_{pk}. The optical detection system already operated in the Lab will be adapted to this cavity in order to investigate a correlation between X-rays and light (visible to NIR) signals if any, by using dielectric/merallic contaminant intentionaly introduced in the cavity dimple region.

AKNOWLEDGMENTS

The authors would like to especially thank M. Arianer,A. Caruette F. Clapier, N. Hammoudi and M. Proust from IPN Orsay, F. Koechlin and B. Mahut for their technical support in cavity preparation during the experimental tests and the paper preparation.

REFERENCES

[1] Proc. of the 1st TESLA Workshop, Cornell university, Ithaca, NY, CLNS 90-1629 (1990),

[2] TESLA - Report 93-18 ; Ed. H.Edwards, M.Tigner, DESY Print, Hamburg (1993),

[3] M. Fouaidy et al., Proc. of the 5th Workshop on RF Superconductivity, DESY, Hamburg, pp 547-576,

[4] J.Arianer et al. IPN Orsay Internal Report Note SFEC T-38 (January 1989),

[5] T.Weiland, NIM 216, pp 329-348 (1983),

[6] W.Weingarten, Proc. of the CAS "RF Engineering for Particle Accelerators", Oxford (UK),1991,CERN 92-03 Vol II,

[7] D.L. Moffat et al., CNLS 89/923 - SRF 890531/3,

[8] S.Bousson, Paris XI Univ. D.E.A (Master) Dissertation - IPN Orsay Report (June 1995).